Stereocomplex Formation through Reorganization of Poly(L-lactic acid) and Poly(D-lactic acid) Crystals

Masahiro Fujita,*,† Tomoharu Sawayanagi,‡ Hideki Abe,‡,§ Toshihisa Tanaka,|| Tadahisa Iwata,⊥ Kazuki Ito,# Tetsuro Fujisawa,#,▽ and Mizuo Maeda†

Bioengineering Laboratory and Chemical Analysis Team, RIKEN Institute, Hirosawa 2-1, Wako, Saitama 351-0198, Japan; Department of Innovative and Engineered Materials, Tokyo Institute of Technology, Nagatsuta 4259, Midori-ku, Yokohama 226-8501, Japan; Faculty of Textile Science and Technology, Shinshu University, Tokida 3-15-1, Ueda, Nagano 386-8567, Japan; Graduate School of Agricultural and Life Sciences, The University of Tokyo, Yayoi 1-1-1, Bunkyo-ku, Tokyo 113-8657, Japan; RIKEN Harima Institute, SPring-8 Center, Kouto 1-1-1, Mikazuki, Sayo, Hyogo 679-5148, Japan; and Graduate School of Engineering, Gifu University, Yanagido 1-1, Gifu, Gifu 501-1193, Japan

Received November 5, 2007; Revised Manuscript Received January 24, 2008

ABSTRACT: The annealing behavior of poly(L-lactic acid) (PLLA) and poly(D-lactic acid) (PDLA) single crystals was investigated in order to reveal the mechanism of chain diffusion in their solid states, below their melting points. The structural changes of the sedimented single-crystal mats on continuous heating were followed in real time by synchrotron small-angle X-ray scattering (SAXS) and wide-angle X-ray diffraction (WAXD) measurements. The single crystal of homopolymer showed a discontinuous thickening at an annealing temperature below each melting point. The experimental evidence indicated that the lamellar thickening occurs by partial melting and recrystallization. On the other hand, it was discovered that the binary mixture of PLLA and PDLA single crystals exhibits a different reorganization at the same annealing temperature. During their lamellar thickening, stereocomplex of PLLA and PDLA appeared. This provides that the molecular chains, which are registered in each homocrystal, mutually diffuse and rearrange. The dominant orientation of the reorganized stereocomplex crystals was the same as that of the original crystals. However, the stereocomplex crystals with the orientation perpendicular to the original ones were also found to form. This peculiar phenomenon supports that the lamellar thickening is due to not chain sliding through the crystal lattice but partial melting and recrystallization.

Introduction

Biodegradable polymers have attracted much attention to solve the problems resulting from the disposal of solid waste, and thus have been studied by many researchers. In particular, the polymers produced from renewable carbon sorces are of interest as attractive alternatives for petroleum-based polymers. For crystalline biodegradable polymer, generally, the morphology of crystalline phase in the material affects both the physical properties and degradability.[1,2] In order to develop the biodegradable material with desirable physical properties and degradability, it is necessary to regulate their morphologies. Understanding the structural change of morphology by external field such as stress and heat as well as crystallization is essential to regulate the material properties. The reorganization by heat treatment, i.e., annealing, brings about enhanced thermal and mechanical properties. Annealing of polymer crystals is thus of interest from both scientific and industrial viewpoints.

Synchrotron radiation X-ray is very powerful to follow in real time such fast dynamic structural changes by annealing. Because the synchrotron small-angle X-ray scattering (SAXS) and wide-angle X-ray diffraction (WAXD) can detect the information on structure from molecular to lamellar length scale in far shorter time, compared with conventional X-ray techniques, the chain motion during thickening process on heating can be evaluated more directly. So far, the thermal behaviors of various polymer crystals[3−6] have been investigated by SAXS and/or WAXD. For example, it was revealed that ultrahigh molecular weight polyethylene (PE) crystal exhibits a doubling of lamellar thickness on heating, which is similar to the discontinuous thickening in oligomer crystals with a thickness that is an integer submultiple of the total chain length.[3] This finding indicates that even polymers with high molecular weight can be easily diffused in the crystal. This thickening has been explained by mutual sliding diffusion between adjacent crystals.[3] Besides PE crystal, similar discontinuous thickening for polyamide and polypivalolactone crystals was previously reported.[7,8]

In our previous papers, the annealing behaviors of poly[(*R*)-3-hydroxybutyrate] (P(3HB)) and its copolymer solution-grown single crystals were revealed at a molecular level by synchrotron radiation X-ray observations.[9−11] Owing to the synchrotron radiation X-ray emitted from an undulator and a high-sensitive CCD camera, we were able to follow the structural changes on heating at tens of milliseconds per frame. Similar to the case of PE crystals, P(3HB) and its copolymer single crystals were found to exhibit a discontinuous lamellar thickening at an annealing temperature below their melting points. It was clearly observed that the thickening progresses in a temperature range, namely, two populations of the original and the reorganized crystals coexist while the former decreases and the latter increases in the thickening. The crystallinity, estimated from the WAXD patterns, first decreased and then recovered during the thickening, although both SAXS and WAXD patterns indicated that the orientation of crystal or molecular chain maintains before and after the thickening. This result was further supported by differential scanning calorimetry (DSC) that endo- and exothermic signals are observed during the thickening. Therefore, we have concluded that the discontinuous lamellar thickening of P(3HB) single crystals is caused by partial melting and recrystallization.[9−11]

* To whom all correspondence should be addressed. Tel: +81-48-467-9312. Fax: +81-48-462-4658. E-mail: mfujita@riken.jp.
† Bioengineering Laboratory, RIKEN Institute.
‡ Tokyo Institute of Technology.
§ Chemical Analysis Team, RIKEN Institute.
|| Shinshu University.
⊥ The University of Tokyo.
RIKEN Harima Institute.
▽ Gifu University.

10.1021/ma7024489 CCC: $40.75
Published on Web 03/19/2008

As a plausible mechanism, we have suggested that the discontinuous lamellar thickening is caused by mutual chain diffusion between the adjacent crystals along the stacking direction and subsequent rearrangement,[10,11] similar to the models proposed previously in some literature.[3,7,12] In this process, however, the molecular stems with helical conformation are probably released from the crystal lattice prior to diffusion due to melting. If subsequent recrystallization takes place immediately, the chains may not relax into random coil state, namely, the chains or chain segments detached from the lattice might be in an intermediate state. Such chain segments possibly diffuse mutually to the space in which the adjacent crystals existed while the orientation maintains.[10,11]

The present study deals with the annealing experiments of poly(L-lactic acid) (PLLA) and poly(D-lactic acid) (PDLA) single crystals by synchrotron SAXS and WAXD, in order to verify our proposed thickening model. For this purpose, we used the binary mixture of PLLA and PDLA single crystals (hereafter abbreviated as PLLA/PDLA). The structural changes of the mixture on heating process were investigated and compared with those of homopolymer crystals. In addition, their thermal properties were examined by differential scanning calorimetry (DSC), similar to our previous works.

Experimental Sections

PLLA and PDLA Single Crystals. The number-average molecular weight (M_n) and the polydispersity (M_w/M_n) of PLLA were 1.3×10^5 and 1.6, respectively. The M_n and M_w/M_n of PDLA were 1.2×10^5 and 1.4, respectively. Single crystals of each polymer were isothermally grown at room temperature from a 0.025(w/v)% acetonitrile solution. The sedimented single crystal mats of each polymer were obtained by filtration of suspension and then dried under vacuum. For the binary mixture PLLA/PDLA sedimented mats, the weight ratio of PLLA and PDLA was 1:1. First, each of the PLLA and PDLA single crystals was grown separately, similar to the case of the homocrystal. After the crystallization, their suspensions were mixed each other, and then the filtration was performed.

Synchrotron SAXS and WAXD Measurements. SAXS and WAXD measurements were carried out at the BL45XU RIKEN Structural Biology Beamline I (wavelength, $\lambda = 0.09$ nm) of SPring-8, Harima, Japan. The camera lengths in the SAXS and WAXD measurements were 2200 mm and 150 mm, respectively. The sample heating apparatus, which is remotely controlled from outside the shielding hutch, was set in the beamline. The single-crystal mats were set in the sample holder and heated from room temperature to around their melting points at a heating rate of 10 °C/min. All two-dimensional (2D) SAXS and WAXD patterns were recorded with a CCD camera (C7300-10-12NR, Hamamatsu Photonics, Japan) coupled with an X-ray image intensifier (V5445P-MOD, Hamamatsu Photonics, Japan), every 1 °C between 145 and 185 °C. The pixel size of CCD camera was 125 μm × 125 μm at the input surface of the detector. The exposure times in the SAXS and WAXD were 29−58 and 18−44 ms, respectively.

Data Analysis. The procedures of data analyses of SAXS and WAXD patterns were the same as those in our previous studies.[9–11] As shown below, the scattering peaks in the 2D SAXS patterns are arced, indicating that the orientation of the sedimented single-crystal mats is distributed. To extract the structural information of the whole system, thus, the 2D SAXS images were converted into one-dimensional (1D) profiles by sector-averaging, as described in ref,[13] with a Rigaku R-AXIS display software package. Subsequently, the Lorentz correction was applied to the azimuthal-average 1D profiles after subtraction of background. The individual scattering peak in the 1D profile was fitted by Gaussian function with IGOR Pro software package (WaveMetrics, Inc.). From the fitting parameters obtained, the long period was calculated. The unit lattice dimension (*a*-axis) was calculated from the peak position, obtained from the fitting of Gaussian function, on the equatorial line scans

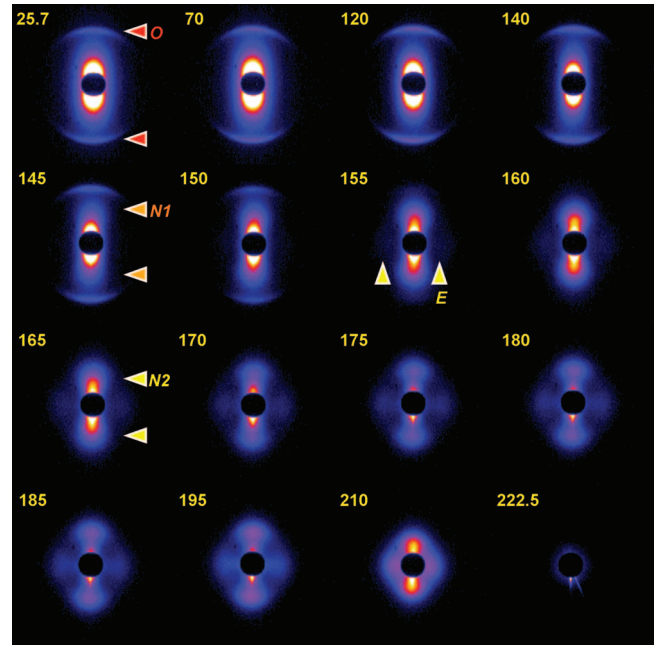

Figure 1. 2D SAXS patterns of the binary mixture of PLLA and PDLA single crystals at elevated temperature, which were taken at the temperatures indicated in the images. The arrowheads indicate the scattering peaks from the original (*O*), and reorganized crystals (*N1* and *N2* on the meridian, and *E* on the equator).

in the 2D WAXD images. For the estimation of overall crystallinity, the 2D WAXD images were converted to the integrated 1D profiles by the same procedure in SAXS analysis. In this case, the averaging over the whole azimuthal angle was performed for all images. Each of crystalline peaks and amorphous scattering was fitted by Gaussian function, and then the total area of crystalline peaks (A_c) and of the amorphous background (A_a) was calculated using the fitting parameters obtained. The crystallinity index, X_c, was thus estimated from the following equation:

$$X_c = \frac{A_c}{A_c + A_a} \times 100 \quad (1)$$

Differential Scanning Calorimetry. Thermal properties of PLLA, PDLA, and PLLA/PDLA single-crystal mats were evaluated by DSC (Perkin-Elmer Pyris 1). The DSC thermograms were obtained under nitrogen atmosphere at the heating rate of 10 °C/min, which was the same rate as that in the synchrotron radiation X-ray measurements.

Results and Discussion

SAXS Measurements. Real-time SAXS measurements on heating at 10 °C/min were performed for solution-grown PLLA/PDLA, PLLA, and PDLA single crystal mats. The 2D SAXS patterns of the binary mixture mats of PLLA/PDLA, obtained at representative temperatures, are shown in Figure 1. For comparison, those of the single-component mats of PLLA and PDLA are also shown in Figure 2. In the SAXS images, the meridian is the lamellar stacking direction in the sedimented mats. Their corresponding 1D profiles are shown in Figure 3. These profiles were averaged within the sector of 90° around the meridian. The profiles from 140 to around 180 °C are shown in this figure.

The red arrowheads (*O*) in Figure 1 indicate a pair of the first-order scattering peak from the binary mixture of as-grown PLLA and PDLA single crystals. No splitting of the scattering peak, i.e., due to two different periodicities, was recognized. As shown in Figure 3, the peak position was around $s = 0.10$ nm^{-1} ($s = 2 \sin \theta/\lambda$, 2θ = scattering angle). This corresponds

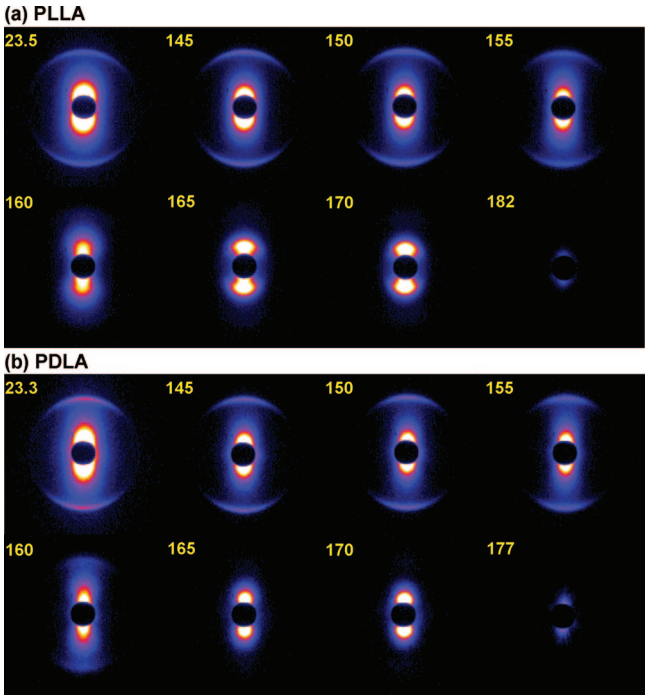

Figure 2. 2D SAXS patterns of the single-crystal mats of PLLA (a) and PDLA (b) at elevated temperature, which were taken at the temperatures indicated in the images.

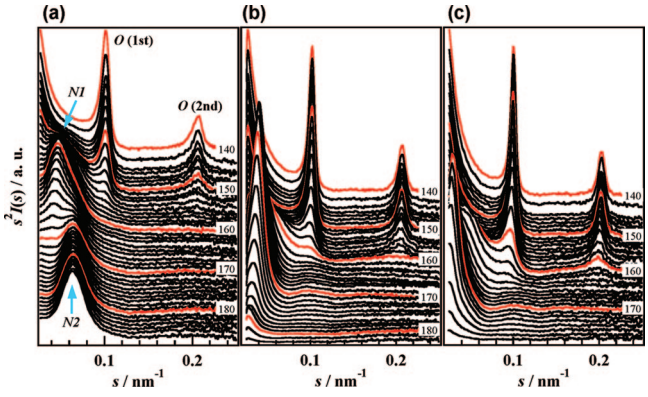

Figure 3. Sector-averaged SAXS profiles of (a) PLLA/PDLA, (b) PLLA, and (c) PDLA single-crystal mats. The profiles from 140 to 186 °C in (a) and from 140 °C to melting in (b) and (c) are shown, with every 10 °C emphasized with red lines.

to the lamellar thickness, L, of 10 nm. Both the first-order scattering peaks from single-crystal mats of individual PLLA and PDLA were also observed at around $s = 0.10$ nm^{-1}. In addition, the scattering peaks from all samples are the same in the peak width, indicating that the stacking regularity of crystals in the binary mats is comparable with those of PLLA and PDLA. It was thus confirmed that, in the binary single-crystal mats, both PLLA and PDLA single crystals with roughly the same thickness stack without any morphological changes.

No remarkable change in the SAXS patterns of PLLA/PDLA was observed up to around 140 °C. When the temperature reached 145–150 °C, a new scattering peak, marked with *N1*, appeared at a lower angle, as shown Figures 1 and 3a. It is indicated that the discontinuous increase of long period takes place at the annealing temperature. Similar to the cases of poly[(*R*)-3-hydroxybutyrate] (P(3HB)) and its copolymer single crystals,[9–11] the new scattering peak became strong as temperature increased, while the original peak (*O*) gradually became weak and finally disappeared at around 160 °C. The corresponding averaged 1D profiles (Figure 3a) demonstrate more

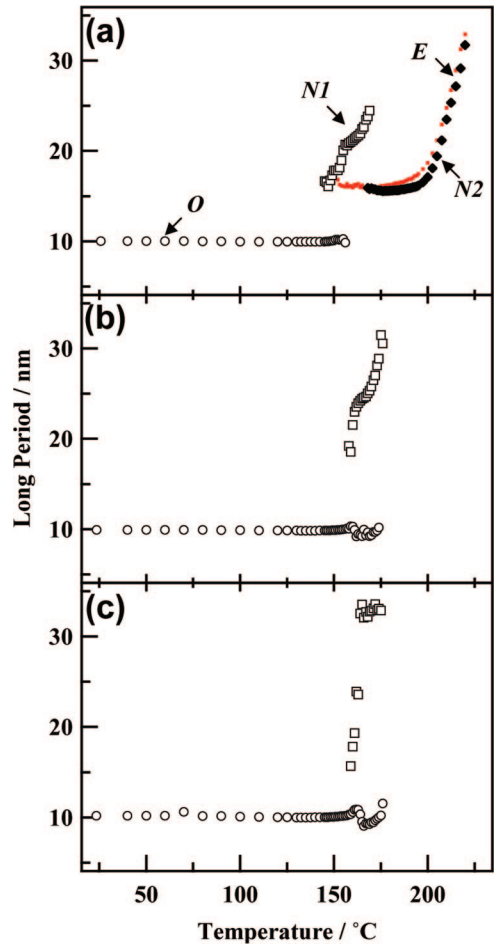

Figure 4. Temperature dependence of long period: (a) PLLA/PDLA, (b) PLLA, and (c) PDLA. In all parts, the circular and square symbols indicate the long periods from the original and reorganized crystals, respectively. In addition, the long period estimated from the scattering on the equator (*E*) is represented with a dot in (a).

distinctly their changes of intensities. The individual single crystal mats of PLLA and PDLA also exhibit the discontinuous thickening at near this temperature, as shown in Figures 2 and 3b,c. Compared with *N1* scattering of PLLA/PDLA, however, their peak widths were sharper.

Further annealing, the peak position from the thickened crystals gradually shifted to lower angles, and the peak intensity became weak with temperature. For the homocrystals of PLLA and PDLA, the scattering peaks diminished at around 180 °C due to complete melting. The binary PLLA/PDLA, however, exhibits quite different behavior. Another scattering peak marked with *N2* observed at a slightly higher angle. The peak intensity of *N2* increased with temperature while that of *N1*decreased and diminished around 170 °C. The scattering peak of *N2* was observed beyond 180 °C without decreasing in intensity (Figure 3). It is evident that the scattering peak *N2* is originated from neither PLLA nor PDLA homocrystals. On the basis of the fact that the *N2* scattering peak is observed up to around 220 °C, this peak is assigned to the long period of stereocomplex crystals.[14,15]

The change in long period for each sample is plotted against temperature in Figure 4. The values were estimated from the integrated 1D SAXS profiles of all data acquired in this study. The original lamellar thickness of all single crystals is roughly the same ($L = 10$ nm) as mentioned above. In the first transition, the long period of the binary PLLA/PDLA increases to 16 nm at around 145 °C, while those of the individual PLLA and PDLA homocrystals also increase discontinuously to 16–19

nm at around 160 °C. For the reorganized homocrystals of individual PLLA and PDLA, their long periods increase continuously up to melting with temperature. On the other hand, the binary PLLA/PDLA single-crystal mats show the second transition of long period at 165–170 °C. At this temperature, the long period appears to decrease discontinuously from 24 to 16 nm. After that, the long period remains constant to 190 °C and increases continuously with temperature.

It should be noted that the discontinuous thickening of the binary mats, namely, the disappearance and emergence of original and new peaks, respectively, occurs at a lower temperature than the cases in the individual PLLA and PDLA homocrystals. The intensity of scattering varies due to a lack and an emergence of stacking periodicity. The formation of stereocomplex crystals might facilitate the lack of stacking periodicity, besides the sporadic disappearance of the original crystals. Furthermore, the faster reorganization to stereocomplex crystals likely brings about the emergence of new periodicity from at a lower temperature. Therefore, the onset of discontinuous thickening of the binary mats may be apparently lower.

Another remarkable feature in the binary PLLA/PDLA crystal mats is the emergence of scattering peak (*E*) on the equator in the 2D pattern shown in Figure 1. This scattering was weaker than that on the meridian, but recognized definitely from around 150 to 220 °C (Figure 1). This scattering peak is thus assigned to the long period of stereocomplex crystals. The equator long period estimated from the peak position was roughly the same as that of *N2* peak on the meridian as shown in Figure 4a. This fact means that the sereocomplex crystals form essentially during the first transition at around 150 °C. The scattering indexed with *N1* shown in Figures 1 and 3a is considered to be the superposition of scatterings from the reorganized α-form[16,17] and stereocomplex crystals, as shown below. Consequently, the second transition of discontinuous decrease in long period is an apparent change just due to melting of the reorganized α-form crystals so that *N2* peak was distinguishable from *N1* peak near 165 °C.

WAXD Measurements. In the SAXS measurements, we could obtain evidence indicating that the stereocomplex crystals form through the reorganization of PLLA and PDLA single crystals. Next, real-time WAXD measurements of PLLA/PDLA, PLLA, and PDLA single-crystal mats were performed in order to examine the changes in crystal structure and crystallinity on heating. The heating rate was 10 °C/min. Figure 5 shows the 2D WAXD patterns of binary PLLA/PDLA crystals, obtained at representative temperatures. Those of PLLA and PDLA homocrystals are also shown in Figure 6. The meridian in the pattern corresponds to the lamellar stacking direction. All the reflections in the WAXD patterns from any sedimented mats, taken at room temperature, were indexed with an orthorhombic unit cell, called α-form.[16,17] The pair of the most intense reflections on the equator is the composition of 110_α and 200_α reflections. Below the first transition temperature, the 2D WAXD patterns remained unchanged. For the binary PLLA/PDLA, a concentric ringlike reflection appeared inside the 110_α/200_α reflections at around 150 °C. On the other hand, no new reflections were observed in the 2D WAXD patterns of homocrystal mats. This ringlike reflection is from stereocomplex crystals and can be indexed as 110_{sc} reflection of stereocomplex on the basis of the crystal structure reported by Cartier et al.[15] The ringlike reflection actually consists of two pairs of arced 110_{sc} reflection perpendicular to each other; one is on the equator and the other on the meridian, supporting that two populations of stereocomplex crystals with the different orientations are formed. On the other hand, the orientation of the α-form crystal remained unchanged. The 110_{sc} was distinguishable from other crystalline reflections of α-form at 150 °C, where the first change

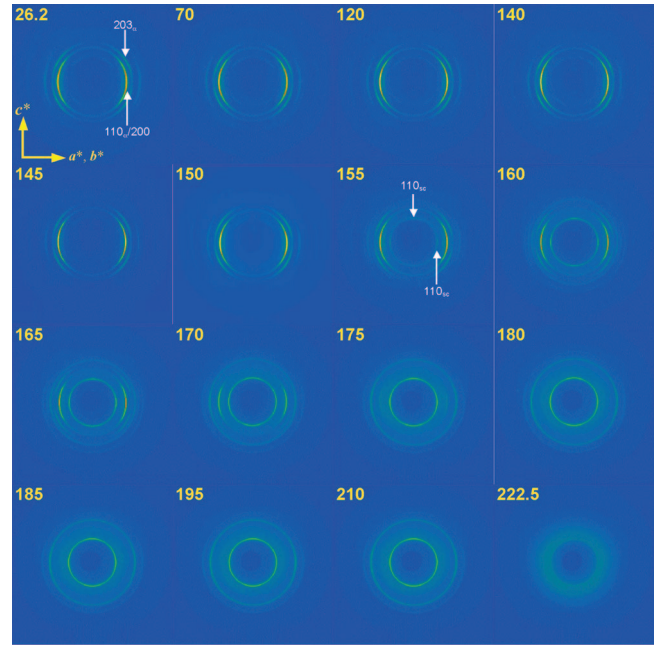

Figure 5. 2D WAXD patterns of the binary mixture of PLLA and PDLA single crystals at elevated temperature, which were taken at the temperatures indicated in the images.

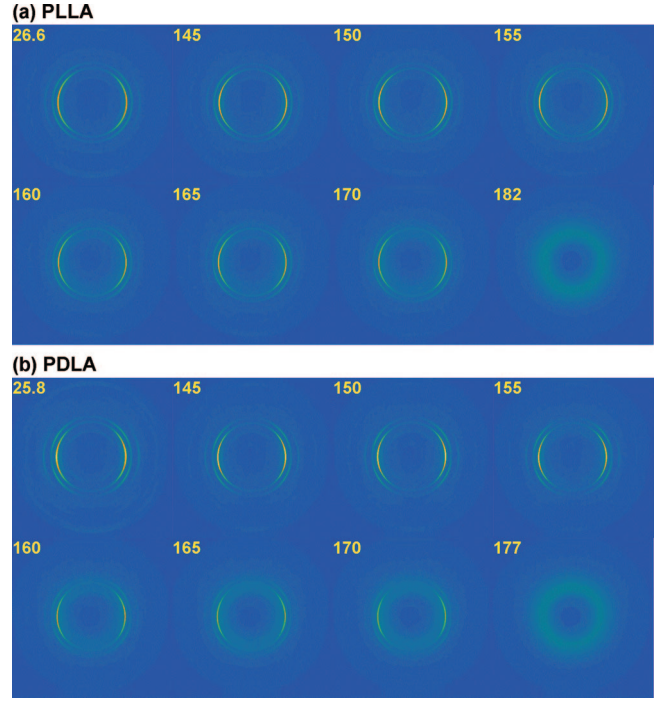

Figure 6. 2D WAXD patterns of the single-crystal mats of PLLA (a) and PDLA (b) at elevated temperature, which were taken at the temperatures indicated in the images.

of long period was observed by SAXS. The WAXD result well supports that the scattering of *N1* on the meridian consists of those from α-form and stereocomplex crystals, and the peak on the equator from only stereocomplex crystals. Above 180 °C, only the reflections from stereocomplex crystals were observed.

Figure 7 shows the line scan profiles on the equator of WAXD image. As can be seen in this figure, the crystal structure of the binary PLLA/PDLA mats drastically changed between 140 °C and around 180 °C, while PLLA and PDLA homocrystals lead to melt without changing their crystal structures. Above 150

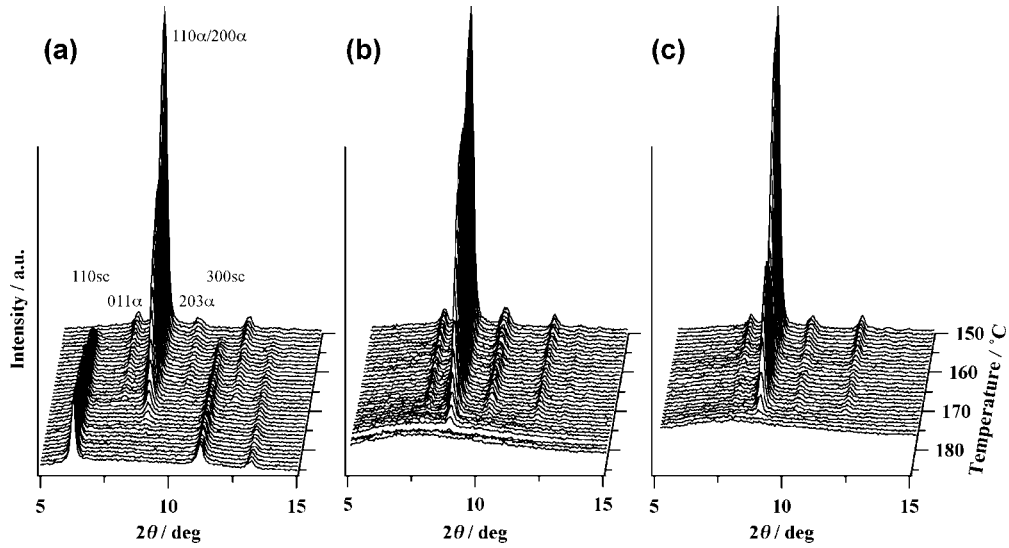

Figure 7. Equatorial line scans of 2D WAXD patterns: (a) PLLA/PDLA, (b) PLLA, and (c) PDLA. The profiles from 150 to 186 °C in (a) and to melting in (b) and (c) are shown. The reflections from stereocomplex are indexed with the crystal structure reported in ref.[15]

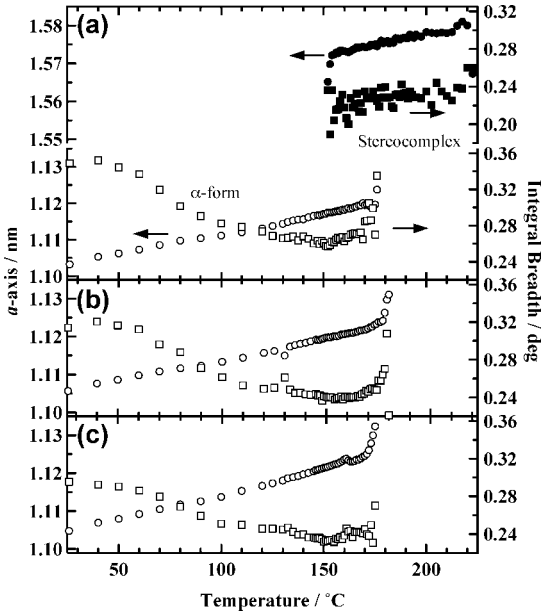

Figure 8. Temperature dependence of *a*-axis (circular symbol) and integral breadth (square symbol). These values are extracted from 110_α/200_α reflection for α-form and 110_{sc} one for stereocomplex. The open and filled symbols represent *a*-axes of α-form and stereocomplex crystals, respectively.

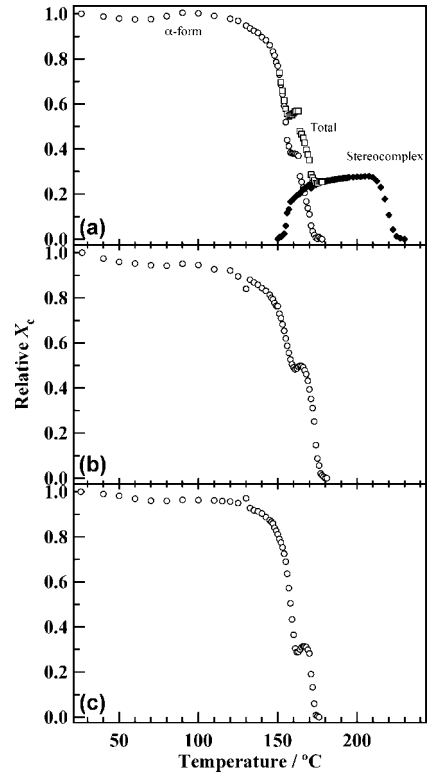

Figure 9. Temperature dependence of crystallinity X_c: (a) PLLA/PDLA, (b) PLLA, and (c) PDLA. Here, X_c represents the relative one to that at room temperature. In (a), the crystallinities of α-form and stereocomplex crystals, separated from the overall one, are also shown.

°C, the reflections from stereocomplex crystals became strong and those from α-form ones became weak (Figure 7a). The α-form reflections could be still detected above 170 °C where *N1* scattering peak in SAXS already disappeared. In this case, the coherency or stacking periodicity of the crystals might be lost by melting.

Temperature dependence of unit cell dimension (*a*-axis) and the integral breadth of reflection were investigated (Figure 8). These values were estimated from $110_\alpha/200_\alpha$ and 110_{sc} reflections, respectively. In all the samples, *a*-axis increased monotonously up to the first transition, indicating that the intermolecular distance expands due to thermal expansion. The monotonous increase of *a*-axis continued just before the complete melting of α-form crystal without showing a contraction upon thickening.[9–11] The integral breadth increased at the onset of the discontinuous thickening, indicating that the lateral crystallite size starts to decrease. Accordingly, the decrease of crystallite size in the lateral direction might lead to the monotonous increase of *a*-axis. For the PLLA/PDLA, the *a*-axis of stereocomplex also showed an increase monotonously with temperature due to thermal expansion.

The temperature dependence of crystallinity, X_c, was investigated. The overall crystallinity was estimated from the circular-averaged 1D WAXD profiles. Figure 9 shows the change in the relative X_c of PLLA/PDLA, PLLA, and PDLA single-crystal mats. In Figure 9a, the crystallinities of α-form and stereocomplex crystals are also shown, which were calculated by substituting the area of crystalline peaks from α-form or stereocomplex for the numerator of eq 1. For all the samples,

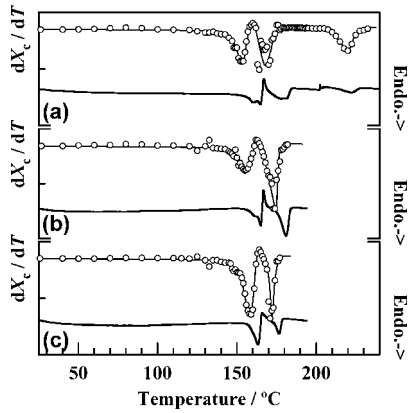

Figure 10. Differential X_c with respect to temperature and DSC curve: (a) PLLA/PDLA, (b) PLLA, and (c) PDLA.

the X_c starts to decrease at the first transition temperature where the discontinuous increase of long period was observed. This decrease stops at 155–165 °C, and then the X_c recovers slightly, indicating that the discontinuous increase is associated with melting of original crystals and recrystallization. The X_cs of PLLA and PDLA homocrystals decrease again after the first transition, and finally drops to zero at around 180 °C due to complete melting. On the other hand, the decrease of the total X_c of PLLA/PDLA stops at a value, due to the formation of stereocomplex crystals. After the α-form crystals disappear due to complete melting at around 180 °C, the total X_c turns to increase gradually. This slow increase is attributed to the crystallization of amorphous chains.

The differential X_c and DSC curves against temperature are shown in Figure 10. This figure demonstrates more clearly that the change in crystallinity on heating corresponds to the thermal properties characterized by DSC. All the DSC curves showed double endotherms and an exotherm between them in the range of 150–180 °C. The lower endotherm and subsequent exotherm at 150–170 °C were assigned to lamellar thickening due to melting of α-form and recrystallization to α-form or to stereocomplex, respectively. The higher endotherm at 170–180 °C is associated with the complete melting of reorganized α-form crystals. The endotherm detected at around 220 °C is undoubtedly due to melting of stereocomplex.

Molecular Motion in Crystal Thickening. In a sedimented single-crystal mat, the lamellar crystals stack along the chain direction while their fold planes are in contact with each other. Despite the space limitation, the crystals are able to thicken along their chain axis, and the thickening is discontinuous as reported previously.[3,7–12] It is thus expected that the discontinuous thickening should be in cooperation with the adjacent crystals. In the stacking lamellar crystals, however, there is a question whether the chains diffuse mutually between the adjacent crystals or not. In contrast to the usual single-component single-crystal mats reported so far,[3,7–12] we used here the binary mixture of PLLA and PDLA single crystals as a special model sample, in order to disclose the molecular motion in the process of lamellar thickening. As a result, the binary mixture of PLLA and PDLA homocrystals exhibits the transition to stereocomplex crystals during their lamellar thickening process (Figure 11), in addition to the thickening with the crystal form unchanged. Although, as shown in Figure 11a, the stereocomplex crystals with two orientations perpendicularly each other were formed through this reorganization, here, we direct our attention to the longitudinal mode (Figure 11a(i)). If the individual crystal of each polymer itself reorganizes to the thicker crystal, we will not surely observe this transition because the stereocomplex consists of two enantiomers of PLLA and

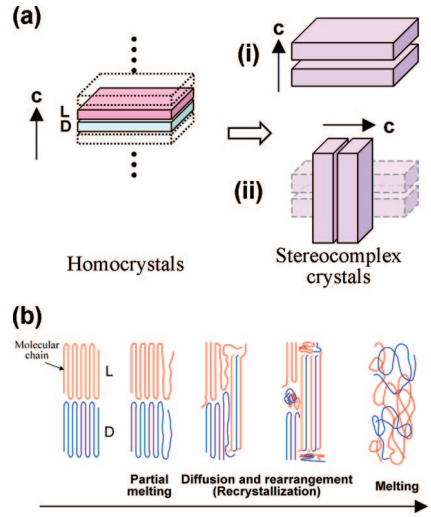

Figure 11. (a) Transition of the binary mixture of PLLA and PDLA single crystals to sterocomplex crystals, and (b) a plausible mechanism of the longitudinal mode (i).

PDLA. Therefore, the transition to stereocomplex crystals proves the molecular mechanism that the lamellar thickening is associated with the mutual chain diffusion between the adjacent crystals and subsequent chain rearrangement side by side, namely the crystals fuse at a molecular level during the lamellar thickening, as illustrated in Figure 11b.

There is still a matter of discussion whether the thickening is due to chain sliding through the crystal lattice or to melting and recrystallization.[3,7–12] As described above, it was revealed that the lamellar thickening of PLLA, PDLA, and PLLA/PDLA is accompanied not only by the endotherm and exthotmerm in heat flow but also by the decrease and slight increase in crystallinity (Figures 9 and 10). In this study, furthermore, we found the reorganization to stereocomplex crystals with two different orientations, as illustrated in Figure 11a. This peculiar phenomenon is hardly explained by chain sliding through the crystal lattice. These evidence suggest that the lamellar thickening is due to melting of original crystal and recrystallization. It is, however, noteworthy that the chain axis before and after the lamellar thickening maintains for PLLA and PDLA crystals, and, even for the binary mixture, the dominant chain axis of the reorganized crystals is consistent with that of the original ones. The chains or chain segments detached from the crystal lattice might orient along the stacking direction as ever, so that the reorganized crystals with the same orientation may grow immediately. The other chains or chain segments that are not incorporated to the crystal lattice will relax further. Such relaxed chains may crystallize on the surface of the surrounding crystal while orienting normal to the chain axis of the parent crystal, like epitaxy, or remain as amorphous state between the reorganized crystals (Figure 11a).

It is well-known that one of the most remarkable features of stereocomplex is its high melting point (220–230 °C) as reported first by Ikada et al.[18] Since then the study on method of preparation of the stereocomplex has been done actively, and many methods for film and fiber materials have been developed.[19–26] In all the methods, the blends of PLLA and PDLA are crystallized from their melt or solution. However, high processing temperatures or removal of solvent are required. Here, we found that the stereocomplex crystals form through the structural transition below the melting point of homocrystals (170–180 °C), in other words, in the solid state. This finding may bring about a new useful method of preparing the stereocomplex material in the bulk without thermal degradation of the molecule. In this study, unfortunately, all original crystals

with α-form did not reorganize to stereocomplex ones exclusively. This is mainly because not all the PLLA and PDLA single crystals stack alternately by the simple method of mixing the suspensions. Furthermore, their single crystals often exhibit multilamellar appearance with spiral growth and so on.[27,28] The regulation of the alternation of crystal stacking as well as the blend ratio may be an important factor to obtain the pure stereocomplex material.

Concluding Remarks

The single crystals of PLLA and PDLA exhibit a discontinuous thickening on heating at an annealing temperature below each melting point, similar to other polymer crystals. The thickening was accompanied not only by the endotherm and exthotmerm in heat flow but also by the decrease and slight increase in crystallinity. When the PLLA and PDLA crystals are in contact with each other, the stereocomplex crystals form through discontinuous crystal thickening. This finding proved that the thickening proceeds by the mechanism that molecular chains mutually diffuse between the crystals and rearrange side by side. We also found that the reorganized crystals have two orientations: parallel and perpendicular to the original crystals. This supports that the lamellar thickening is due to not chain sliding through the crystal lattice but partial melting and recrystallization. Furthermore, the present study suggests a new method to make the stereocomplex materials in solid state.

Acknowledgment. This work has been partly supported by grants of Ecomolecular Science Research from RIKEN Institute. The making of the sample heating apparatus was supported by a DRI Director's Grant from RIKEN Institute (to M.F.). The authors also thank to Yamamoto-seisakujo, Japan, and KEYENCE Co. Ltd., Japan, for making the sample heat unit and its remote control unit, respectively.

References and Notes

(1) Doi, Y. *Microbial Polyesters*; VCH Publishers: New York, 1990.
(2) Sudesh, K.; Abe, H.; Doi, Y. *Prog. Polym. Sci.* **2000**, *25*, 1503–1555.
(3) Rastogi, S.; Spoelstra, A. B.; Goossens, J. G. P.; Lemstra, P. J. *Macromolecules* **1997**, *30*, 7880–7889.
(4) Rastogi, S.; Kurelec, L.; Lemstra, P. J. *Macromolecules* **1998**, *31*, 5022–5031.
(5) Krüger, K. N.; Zachmann, H. G. *Macromolecules* **1993**, *26*, 5202–5208.
(6) Wang, Z. G.; Wang, X. H.; Hsiao, B. S.; Phillips, R. A.; Medellin-Rodriguez, F. J.; Srinivas, S.; Wang, H.; Han, C. C. *J. Polym. Sci., Part B: Polym. Phys.* **2001**, *39*, 2982–2995.
(7) Dreyfuss, P.; Keller, A. *J. Macromol. Sci., Phys.* **1970**, *B4*, 811–836.
(8) Kawaguchi, K.; Murakami, S.; Kajiwara, K.; Katayama, K. *J. Polym. Sci., Part B: Polym. Phys.* **1989**, *27*, 1463–1476.
(9) Fujita, M.; Sawayanagi, T.; Tanaka, T.; Iwata, T.; Abe, H.; Doi, Y.; Ito, K.; Fujisawa, T. *Macromol. Rapid Commun.* **2005**, *26*, 678–683.
(10) Sawayanagi, T.; Tanaka, T.; Iwata, T.; Abe, H.; Doi, Y.; Ito, K.; Fujisawa, T.; Fujita, M. *Macromolecules* **2006**, *39*, 2201–2208.
(11) Sawayanagi, T.; Tanaka, T.; Iwata, T.; Abe, H.; Doi, Y.; Ito, K.; Fujisawa, T.; Fujita, M. *Macromolecules* **2007**, *40*, 2392–2399.
(12) Statton, W. O. *J. Appl. Phys.* **1967**, *38*, 4149–4151.
(13) Kumaraswamy, G.; Verma, R. K.; Kornfield, J. A.; Yeh, F.; Hsiao, B. S. *Macromolecules* **2004**, *37*, 9005–9017.
(14) Okihara, T.; Tsuji, M.; Kawaguchi, A.; Katayama, K.; Tsuji, H.; Hyon, S. H.; Ikada, Y. *J. Macromol. Sci.-Phys.* **1991**, *B30*, 119–140.
(15) Cartier, L.; Okihara, T.; Lotz, B. *Macromolecules* **1997**, *30*, 6313.
(16) De Saintis, P.; Kovacs, A. J. *Biopolymers* **1968**, *6*, 299–306.
(17) Hoogsten, W.; Postema, A. R.; Pennings, A. J.; ten Brinke, G.; Zugenmaier, P. *Macromolecules* **1990**, *23*, 634–642.
(18) Ikada, Y.; Jamshidi, K.; Tsuji, H.; Hyon, S.-H. *Macromolecules* **1987**, *20*, 904–906.
(19) Tsuji, H.; Horii, F.; Hyon, S.-H.; Ikada, H. *Macromolecules* **1991**, *24*, 2719–2724.
(20) Tsuji, H.; Hyon, S-H.; Ikada, H. *Macromolecules* **1991**, *24*, 5651–5656.
(21) Tsuji, H.; Ikada, Y.; Hyon, S.-H.; Kimura, Y.; Kitao, T. *J. Appl. Polym. Sci.* **1994**, *51*, 337–344.
(22) Serizawa, T.; Yamashita, H.; Fujiwara, T.; Kimura, Y.; Akashi, M. *Macromolecules* **2001**, *34*, 1996–2001.
(23) Bourque, H.; Laurin, I.; Pézolet, M.; Klass, J. M.; Lennox, R. B.; Brown, G. R. *Langmuir* **2001**, *17*, 5842–5849.
(24) Takasaki, M.; Ito, H.; Kikutani, T. *J. Macromol. Sci., Part B: Phys.* **2003**, *B42*, 403–420.
(25) Tsuji, H.; Nakano, M.; Hashimoto, M.; Takashima, K.; Katsura, S.; Mizuno, A. *Biomacromolecules* **2006**, *7*, 3316–3320.
(26) Zhang, J.; Tashiro, K.; Tsuji, H.; Domb, A. J. *Macromolecules* **2007**, *40*, 1049–1054.
(27) Miyata, T.; Masuko, T. *Polymer* **1980**, *38*, 4003–4009.
(28) Fujita, M.; Doi, Y. *Biomacromolecules* **2003**, *4*, 1301–1307.

MA7024489